

# Investigating the main reasons for the tragedy of large saline lakes: Drought, climate change, or anthropogenic activities? A call to action

Ehsan Foroumandi<sup>a</sup>, Vahid Nourani<sup>a,c,\*</sup>, Sameh Ahmed Kantoush<sup>b</sup>

<sup>a</sup> Centre of Excellence in Hydroinformatics and Faculty of Civil Engineering, University of Tabriz, Iran

<sup>b</sup> Water Resources Research Centre, Disaster Prevention Research Institute, Kyoto University, Japan

<sup>c</sup> Near East University, Faculty of Civil and Environmental Engineering, Near East Boulevard, 99138, Nicosia, via Mersin 10, Turkey

## ARTICLE INFO

### Keywords:

Drought  
Climate change  
Anthropogenic activities  
Remote sensing  
Wavelet coherence  
Lake urmia

## ABSTRACT

Climate change, drought, and anthropogenic effects are among the main drivers causing alterations in natural resources one of which is the lake level (LL) of large saline lakes, which are mainly located in arid and semi-arid regions. As an urgent need to manage natural resources, this study focuses on determining the significant reasons for the shrinkage problem of saltwater lakes. To this end, the long-term severity and frequency of droughts from 2003 to 2020 and their spatiotemporal distribution in the Lake Urmia Basin (the second largest saline lake on Earth) were investigated based on the normalized difference vegetation index (NDVI) anomaly. Thereafter, monthly soil moisture, evapotranspiration, land surface temperature (LST), LL, NDVI, and precipitation time series were collected, Boolean images were used to generate drought frequency maps, and Mann-Kendall trend test techniques and wavelet transform coherence (WTC) were used to determine the impacts of anthropogenic activities and climate change on the region. The results indicated that the basin had only non-drought and mild drought conditions and did not experience moderate, severe, or very severe droughts. The results indicated that the mild drought indices covered 80% of the total area and were exposed for more than seven years. Pearson correlation analysis indicated that the primary reason for the drought was temperature anomalies ( $r = -0.68$ ) in the basin. The annually changing drought conditions in the basin revealed human effects on the basin. The results indicated a statistically significant positive trend in evapotranspiration time series, which was a reason for the LL decline. Thereafter, wavelet coherence was employed to delve deeper into the correlation between LL and the hydro-environmental datasets. The increasing vegetation cover in the situation that precipitation, land surface temperature, and soil moisture had stable conditions as well as common periodicities between the hydro-environmental variables, and the abrupt change points in significant periodicities revealed that anthropogenic activities in terms of agricultural expansion had increased in the basin. Besides, the annually changing condition of drought in the basin is also an indicator of anthropogenic activities that affect the environment. The differences in the spatial distribution of the NDVI maps also indicated that people living in the western, eastern, and southern regions of the basin had cultivated more land.

## 1. Introduction

Lake-level (LL) decline is among the common environmental problems in large lakes and seas across the world (e.g., Alivernini et al., 2018; Dehghanipour et al., 2020; Ye et al., 2020). The problems related to lakes can be categorized into climate change, droughts, and anthropogenic impacts. Saltwater lakes with an approximately 82,676 km<sup>3</sup> total volume account for 41% of the total global lakes and are mostly located in semiarid and arid basins (Wurtsbaugh et al., 2017). Due to the critical roles of these lakes in natural processes, it is vital to investigate the main

reasons for this problem. LLs of large saline lakes across the world are declining at an alarming rate, which threatens economic activities, human health, and habitats. The oldest known impact of saline lake desiccation on humans was in the Tarim basin, which led to the collapse of a kingdom (Mischke et al., 2017). Fig. 1 presents some of the large saline lakes (formerly larger than 250 km<sup>2</sup>) that have water-related problems due to drought, climate change, and/or anthropogenic activities. For example, the Aral Sea lost 74% of its area due to agricultural activities, Owens Lake in California disappeared by 1940, and the Dead Sea lost a great deal of inflowing water due to excessive usage of fresh

\* Corresponding author. Mailing address: Faculty of Civil Engineering, University of Tabriz, 29 Bahman boulevard, Tabriz, Iran.  
E-mail address: [nourani@tabrizu.ac.ir](mailto:nourani@tabrizu.ac.ir) (V. Nourani).

<https://doi.org/10.1016/j.jaridenv.2021.104652>

Received 8 August 2021; Received in revised form 10 September 2021; Accepted 14 September 2021

Available online 11 October 2021

0140-1963/© 2021 Elsevier Ltd. All rights reserved.

water for drainage (Wurtsbaugh et al., 2017). The main difference between exploring a fresh-water lake and a saltwater lake are the outflows from the lake. The water of freshwater lakes can directly be used for drinking, agricultural purposes and other activities but the water of saline lakes are not appropriate for these utilizations. Lake Urmia, as the second largest saltwater lake on Earth and the largest lake in Iran, has experienced a rapid LL decrease during the past two decades. Some researchers have attempted to determine the reasons for the decline by studying drought in the basin (e.g., Amirataee et al., 2018; Lashkari et al., 2021). Several studies have argued that human land and water use were the primary reasons for the problem (e.g., Khazaei et al., 2019; Foroumandi et al., 2021). On the other hand, other studies have proposed that dam construction was the leading cause of the decline, although this was rejected in a paper that observed the same trend in headwater areas (Fathian et al., 2014). According to previous studies, due to the low quality of the water, which makes it inappropriate for drinking and agricultural activities, the special topography of the region, which makes any direct outflow impossible, and reviews on groundwater gradient directions, which indicate no considerable volume of flows, the only outflow from the lake is through evaporation (Hassanzadeh et al., 2012). The significant reasons for the problems related to saltwater lakes can be traced to drought, climate change, and anthropogenic activities.

Drought, as one of the potential reasons for the problems of salt water bodies, is a devastating environmental disaster that occurs in all climatic zones. The reduction in precipitation volume in the crop-growing season, increasing temperature, and human activities are among the important reasons for droughts (Zhao et al., 2020). Meteorological drought, agricultural drought, hydrological drought, and socio-economic droughts are four major groups to classify droughts. Researchers use various methods and indices to monitor and study droughts. Assessment of vegetation health and condition changes by remote sensing (RS) tools is widely used for drought detection. The normalized difference vegetation index (NDVI) is one of the most frequently used vegetation indices to monitor environmental situations (e.g., Fujihara et al., 2020; Nourani et al., 2021).

Currently, climate change is among the most significant reasons for variations in the environment. Investigation of the impacts of climate

change is crucial in studying hydrologic variables, including studies related to lakes. There is a significant demand to study climate change in lake basins due to its harsh effects on the environment. Drivers and climate change indicators are complicated and can be traced by investigating hydro-environmental variables, such as temperature, precipitation, evapotranspiration (ET), and soil moisture (SM). In recent years, trend analysis has been used to determine the impacts of climate change and human activities on the environment. The intensification of hydrologic cycles is one of the most apparent effects of climate change (Zhang et al., 2009). In this regard, Different statistical methods have been used to study potential trends in time series. For example, Danandeh Mehr and Vaheddoost (2020) used trend test techniques to investigate drought across Ankara, Turkey. In another study, Danandeh Mehr et al. (2021) utilized two new and two classic methods to explore long term temperature and precipitation time series. As a statistical method, the Mann-Kendall (MK) trend test is one of the most widely used approaches in hydro-environmental and climate studies (e.g., Nyikadzino et al., 2020; Zhai et al., 2020).

To determine the impacts of climate change and anthropogenic activities on the environment, studying the relationships between hydro-environmental variables can be of great help. Previous studies have applied correlation coefficients such as Pearson's correlation (PCC) and linear correlation to investigate the relationships between drought indices, climatic factors, and hydrologic variables (e.g., Nanzad et al., 2019; Khazaei et al., 2019). These coefficients can provide useful insights into the relationships; however, they are too simple to reflect the changes or proper investigation of the relationships between naturally related variables (Liu et al., 2017). Wavelet transform coherence (WTC) is a mathematical tool that analyses the linkage between two time series in both the frequency and time domains. It combines the cross-spectrum with wavelet transform; consequently, it is able to determine characteristics in the relationship between two time series. It is suggested to utilize WTC, which first normalizes the wavelet power spectra and then measures the cross-correlation of the given string (Liu et al., 2019; Elsanabary et al., 2021).

Large salt water lakes around the world, including Lake Urmia, are experiencing many problems. As an urgent need to manage water resources, the current study uses remote sensing tools, Mann-Kendall

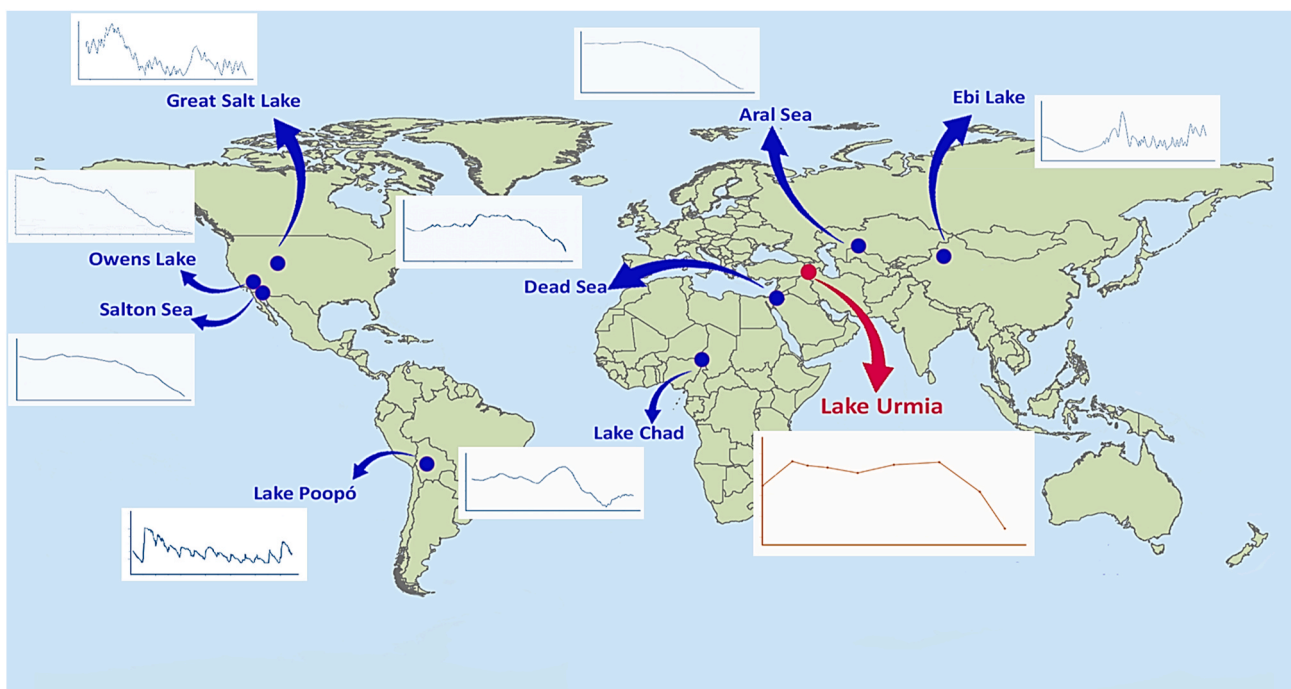


Fig. 1. Some of the world's large saline lakes with water-related problems.

trend tests, and wavelet transforms to investigate the hydrologic and environmental situation in the Lake Urmia Basin, which is the second largest saline lake in the world. Long-term spatiotemporal drought, climate change, and anthropogenic impacts are detected and monitored in the Lake Urmia basin, and their characteristics are traced using hydroclimatological attributes. To the best of our knowledge, this is the first time that spatiotemporal problems of large saltwater lakes have been investigated at this scale at the same time to determine significant problems.

## 2. Materials and methods

### 2.1. Case study

Lake Urmia, located between  $37^{\circ}4'$  and  $38^{\circ}17'$  latitude and  $45^{\circ}13'$  to  $46^{\circ}$  longitudes (Fig. 1), is a hypersaline lake. The lake was the second largest saline lake on Earth before September 2010, and it is the largest lake in Iran. The lives of more than 6 million people depend on their relationship with the lake (Delju et al., 2013). In recent years, a quarter of the lake has changed to saline regions. Variation in LL was 7 m in a lake that was 16 m deep from 1992 to 2020. The basin of the lake is surrounded by mountains, and the climate is cold and continental. Annual precipitation rate in the basin is 341 mm, temperature fluctuation is  $62^{\circ}\text{C}$ , and the maximum and minimum temperatures are  $39^{\circ}\text{C}$  and  $-23^{\circ}\text{C}$ , respectively [Iran Meteorological Organization (IRIMO)]. The area of the lake was about 5650 and 4610  $\text{km}^2$  in 1998 and 2001, respectively and the normal catchment area of Urmia lake is about 51, 676  $\text{km}^2$  which means 3.15% of the entire country [Urmia Lake Basin Integrated Water Resources Management (IWRM)].

### 2.2. Proposed methodological approach

The current study proposed an innovative approach, presented in Fig. 2, to investigate the main reasons for LL decline in large saline lakes with a focus on Lake Urmia, and includes four major steps:

I Data collection: RS tools were utilized to create the NDVI, LST, SM, ET, and precipitation time series. LL data were provided by the Urmia Lake Restoration Program.

- II Calculations of drought indices and indicators: NDVI, LST, and precipitation anomalies were calculated as the differences between the value of each year and the average value.
- III Drought severity and frequency map: Investigating classified spatiotemporal drought severity and frequency maps and the main reason for the drought.
- IV Analysing trends: The Mann-Kendal trend test was used to determine potential trends in the monthly hydrometeorological time series.
- V Correlation analysis: WTC was used to analyse the relationships between LL and LST, precipitation, ET, and NDVI datasets to determine the impacts of anthropogenic activities and climate change on the lake-level problem of Lake Urmia.

In the coming sections, each step is elaborated as the basis for the study.

### 2.3. Data collection

NDVI is a popular index that is used to study vegetation cover over land. The NDVI is a normalized parameter that ranges between  $-1$  and  $1$ . Closer values to  $1$  indicate denser and fresher vegetation (Pettorelli et al., 2005). Monthly NDVI data as a remotely sensed index were collected using the product of MODIS (MOD13A1v006). Additionally, the MOD11A1 product of MODIS was used to generate the monthly LST time series. LST is a crucial parameter in the energy flux between the Earth and atmosphere (Sobrino et al., 1991).

Launched in 1997, TRMM carries several instruments, including the Visible Infrared Radiometer (VIRS), TRMM Microwave Imager (TMI), Cloud and Earth Radiant Energy Sensor (CERES), Lightning Imaging Sensor (LIS), and Precipitation Radar (PR). Using remote sensing satellites, ground rainfall gauges, and infrared sensors, TRMM utilizes various methods to generate precipitation time series (Keikhosravi Kiany et al., 2020). The TRMM product was used to extract monthly precipitation data in the Lake Urmia basin.

The monthly ET and SM time series were generated using the Global Land Data Assimilation System (GLDAS) model, which provides data from 1984 by combining satellite observations and land surface models named Noah, VIC, Mosaic, and CLM. Previous studies have shown that the GLDAS dataset is sufficiently accurate for hydrologic and environmental studies in Iran (Moghim, 2018).

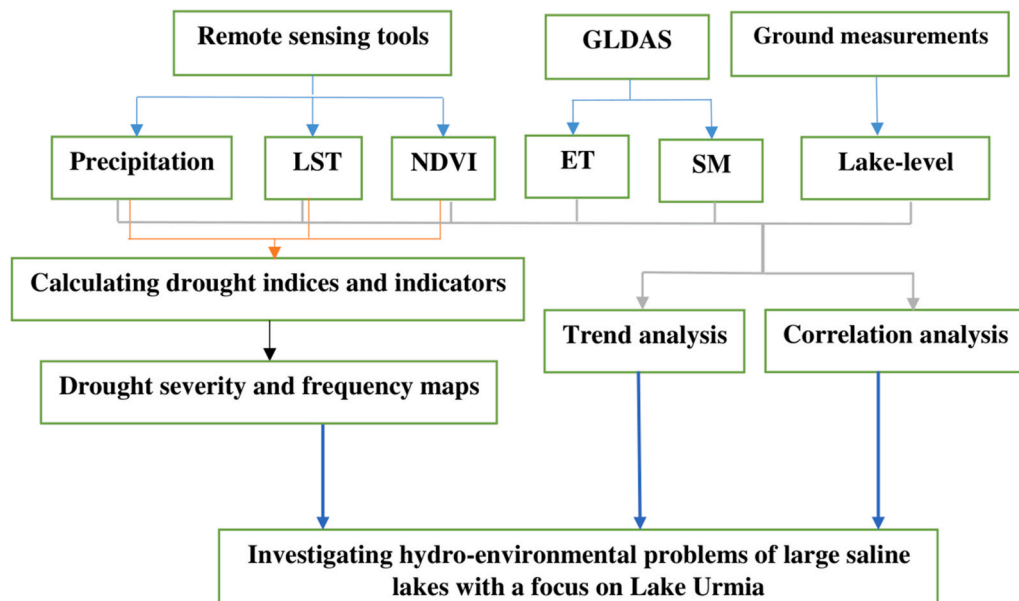


Fig. 2. Schematic of the proposed methodology to investigate the main reasons for the lake-level decline in large saline lakes.

## 2.4. Calculation of drought indices and indicators

The current study utilized NDVI anomaly to study drought severity and frequency over the Lake Urmia basin. The positive values of the NDVI anomaly indicate normal conditions, and negative values show severe drought conditions. To calculate the standardized NDVI anomaly percentage for each year in each pixel, first, the mean NDVI of the period (crop-growing season) was computed, and then the overall NDVI mean ( $\overline{NDVI}$ ) was calculated for 2003–2020 for each pixel (Nanzad et al., 2019):

$$\overline{NDVI} = \frac{\sum_{i=1}^n NDVI_{mean(i)}}{n} \quad (2)$$

where  $NDVI_{mean(i)}$  is the mean NDVI for each year from 2003 to 2020, and  $n$  is the number of years, which equals 17 years. Thereafter, the standardized NDVI anomaly percentage could be derived for each pixel in each year as:

$$NDVI_{anomaly(i)} = \frac{NDVI_{mean(i)} - \overline{NDVI}}{\overline{NDVI}} \times 100 \quad (3)$$

where  $NDVI_{anomaly(i)}$  is the NDVI anomaly for each year during the growing season for each pixel. NDVI anomalies should then be averaged to calculate the mean NDVI anomaly over 18 years.

The LST and precipitation anomalies were also calculated in the same way to determine the primary reasons for drought by analysing the correlation between them and NDVI anomalies.

## 2.5. Drought severity and frequency

Drought severity classification was performed in this study based on the NDVI anomaly classification scheme, as shown in Table 1. The scheme classifies drought severity into normal, mild drought, moderate drought, severe drought, and very severe drought.

Drought frequency was studied by interpreting each of the drought maps as a Boolean image. For each year and drought severity class, a binary map was generated; a total of 18 Boolean annual maps were generated for each category. The Boolean logic math tool interprets the inputs as Boolean values, where zero values are considered false and nonzero values are considered true. Here, a Boolean map indicates whether a specific kind of drought severity occurred in a pixel. Then, the frequency of each class was obtained by adding 17 binary maps at each pixel.

## 2.6. Mann-Kendall trend tests

The Mann-Kendall test is a well-known trend test analysis in various study fields since no specific statistical distribution is needed to use the test (Figueira Branco et al., 2019). The original version of the test (MK1) is used to study the time series with no significant autocorrelation.

High positive and low negative MK statistical values denote statistically significant increasing and decreasing trends, respectively. The significance of a trend is determined according to the probability value (p-value). The null hypothesis of no trend in the MK test is not acceptable provided that the p-value becomes less than the predefined significance level (here,  $\alpha = 5\%$ ) or greater than the confidence level (95%)

**Table 1**  
Drought severity classification (Nanzad et al., 2019).

Drought severity class	NDVI anomaly percentage
Normal (non-drought)	Above 0
Mild drought	0 to -10
Moderate drought	-10 to -25
Severe drought	-25 to -50
Very severe drought	Below -50

(Rashid et al., 2015).

The results of the trend analysis may be misguided if the time series contains significant autocorrelation and seasonality patterns (Nalley et al., 2012). Autocorrelation analysis is needed to avoid this problem. The Lag-1 autocorrelation coefficient is used to examine the significance of autocorrelation. If the dataset includes a significant autocorrelation, it is suggested to use the prewhitening MK test (MK2), by which, first, the autocorrelation should be removed from the time series and then the MK test should be applied (e.g., Yue et al., 2002; Mullick et al., 2019; Mallick et al., 2021).

## 2.7. Correlation analysis

In this study, the correlation between the drought indices and temperature and precipitation anomalies was studied to determine the main reasons for drought in the basin. In addition, the correlation between hydroclimatological factors and LL was analysed to investigate the main reasons for LL decline. In this regard, the PCC test was used to study the correlation between the drought indices and climatic factors. The WTC was then employed to reflect the direction and degree of correlation between the hydro-environmental variables and LL. The WTC is used to examine the changing characteristics of two given time series and to investigate coupled oscillations in both the time and frequency domains (Torrence and Compo, 1998). The current study used the Morlet wavelet function due to its applicability for hydro-environmental time series investigations (Grinsted et al., 2004).

The phase differences were plotted on WTC graphs by arrows directing in terms of radians. A positive correlation (in-phase) between two given time series is indicated by an arrow pointing up or to the right with  $x$  leading. An arrow pointing to the left shows a negative correlation (anti-phase). In a WTC graph, the period at the 5% significance level in which the time series has a high correlation is shown with thick black lines and Cone of Influence (COI); where the impacts of edges are denied, this is shown with a thick counter line (Torrence and Compo, 1998).

When investigating PCC, if the value of the coefficient becomes greater than zero, the two variables have a positive relationship. For values less than zero, the variables have a negative relationship, and a zero value indicates that the variables do not have any relationship (Tong et al., 2017).

## 3. Results and discussion

The current study used remote sensing tools and ground measurements to develop long-term spatial maps for alterations. The developed maps were utilized to assess the impacts of drought, climate change, and anthropogenic activities on Lake Urmia. At the first stage, drought spatiotemporal severity maps were investigated, and the main reasons for drought in the basin were determined. At the next step, trend tests were performed to study potential trends in hydroclimatological time series in the basin. Finally, WTC was used to delve deeper into the relationships between different variables and the LL of the lake.

### 3.1. Data analytical results

The mean LST and precipitation distribution were extracted to study the spatial relationships between the factors and drought frequency and severity maps. The datasets were calculated for each year and each pixel in the basin during the crop-growing seasons. Then, the mean values were computed for all study years for each pixel. Thereafter, the final data were acquired as a statistic for the entire basin for each year and all years. The mean LST for each year in the entire basin fluctuated between 40 °C for 2006 as the coldest year, and 49 °C for 2014 as the warmest year. The mean LST for 2003–2020 during the growing seasons for each pixel, as indicated in Fig. 3 (a), ranged from 26 °C to 56 °C. The basin had approximately 30 °C temperature fluctuations in a pixel-by-pixel



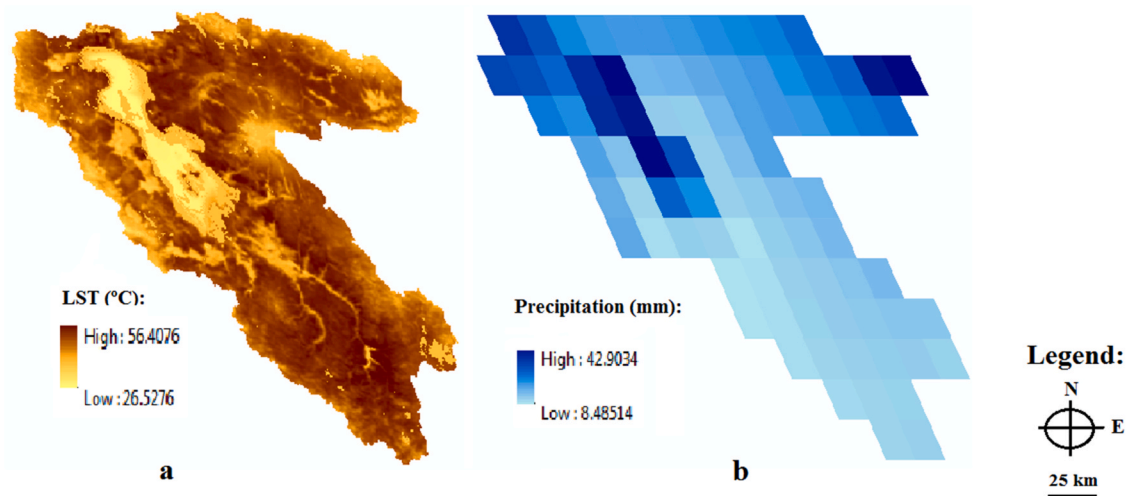


Fig. 3. Spatial distribution map of (a) mean LST and (b) mean precipitation during crop growing seasons in 2003–2020.

comparison, and the mean LST in the basin for 17 years was approximately 45 °C during the growing seasons. According to the results, 2017, with an 11 mm average monthly precipitation, was the driest year, and 2004, with 26 mm, was the wettest year. Additionally, the mean precipitation for 2003–2020 during the growing seasons, as indicated in Fig. 3 (b), for each pixel, ranged between 8 mm and 43 mm, with 35 mm of precipitation fluctuations because of the semiarid climate of the region, and the mean precipitation in the entire basin was 17 mm. The

northern pixels of the map had more precipitation than the southern pixels, which were mainly the pixels over the lake.

The monthly time series were employed for 2003–2020 (216 months in total), as shown in Fig. 4, to study the relationships between the time series of hydrologic and atmospheric variables using the WTC and their potential trends.

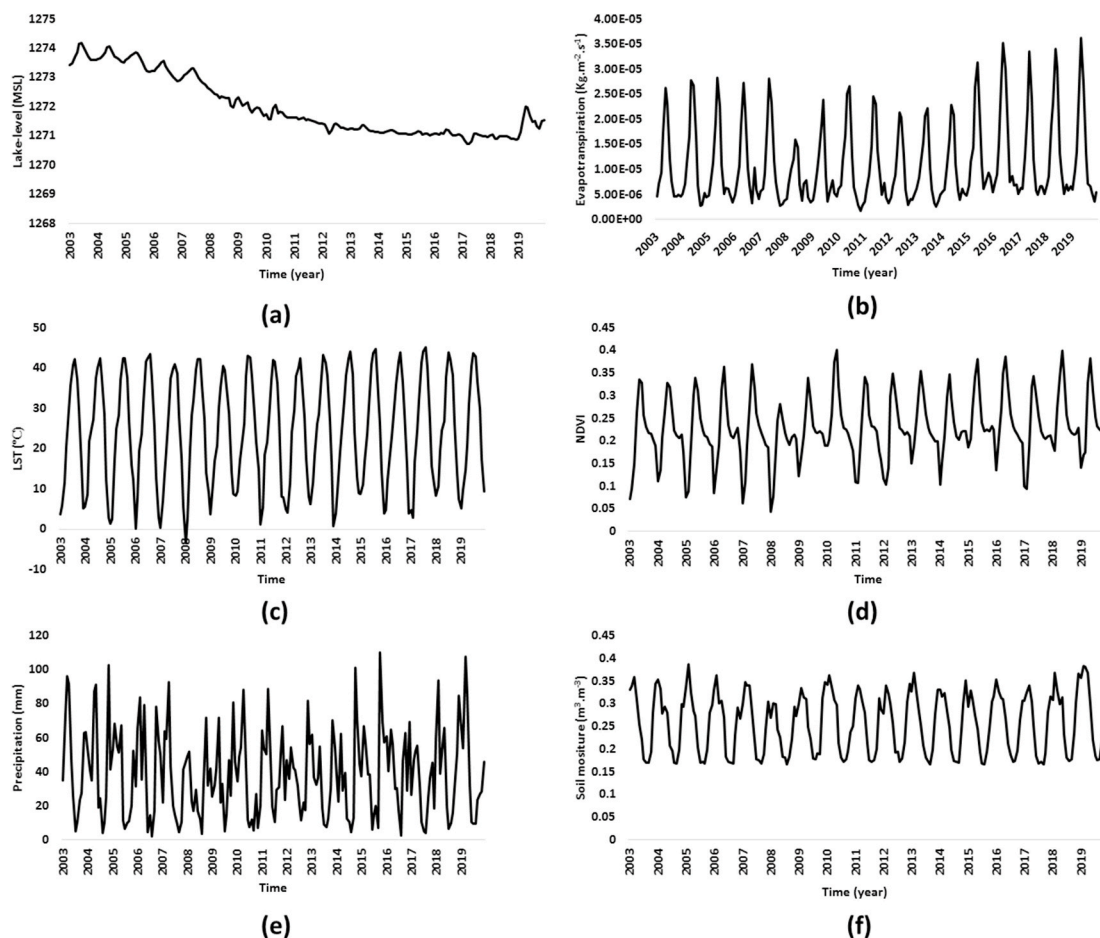


Fig. 4. The monthly time series of hydro-environmental variables in the Lake Urmia Basin during 2003–2020; (a) lake level, (b) evapotranspiration, (c) LST, (d) NDVI, (e) precipitation, and (f) soil moisture.

### 3.2. Drought zoning

Drought monitoring in the Lake Urmia Basin was performed by generating drought maps using the NDVI anomaly from 2003 to 2020, and the results are presented in Fig. 5 and Table 2. According to the results, in the past 17 years, the percentage of areas that have suffered from moderate, severe, or very severe drought was less than 0.01%. The high rate of the regions affected by mild drought illustrated abnormal environmental conditions in the basin in recent years. The years most affected by drought among the past 17 years were 2008 and 2009, with 91.6% and 84.0% of the area, respectively. Additionally, some parts of the basin experienced mild drought in almost all study years, a sign of long-term drought. The percentage of the areas affected by drought in 9 years was more than 50%, while for only two years, more than 80% of the total area was identified as areas with normal conditions. In addition, only two years showed mild drought conditions in more than 80% of the entire area. Among the study years, 2018 and 2019, with 84.6% and 82.1% of the total area, respectively, were considered wet years and years less affected by drought. The results indicated that long-term mild drought conditions ended in 2018 in the basin. The unsteady and sudden change in drought conditions is an indicator of the effects of human activities in the basin, which triggered the switching of drought levels with high spatiotemporal variations.

Drought frequency is defined as the number of years that a specific class of drought has occurred in a pixel. Boolean images were used to investigate drought conditions in the pixels for each year as 0 for not occurred and 1 for occurred. According to Table 2, only the mild drought class occurred in the Lake Urmia Basin in the past 17 years; therefore, one frequency map was generated for this class, as shown in Figs. 6 and 7. According to Fig. 6, the northern and northeastern parts of the basin experienced more drought frequency over the past 17 years. Fig. 4 also shows that during the years with a low area percentage of droughts, such

**Table 2**

The percentage of drought-affected areas in the drought severity classes.

Year	Normal	Mild	Moderate	Severe	Very severe
2003	65.1450	34.8387	0.0108	0.0028	0.0027
2004	68.6097	31.3764	0.0072	0.0029	0.0038
2005	56.1109	43.8773	0.0063	0.0032	0.0023
2006	37.7232	62.2656	0.0049	0.0031	0.0032
2007	72.1499	27.8378	0.0068	0.0032	0.0023
2008	08.3764	91.6122	0.0050	0.0019	0.0045
2009	15.9650	84.0281	0.0023	0.0014	0.0032
2010	42.5199	57.4702	0.0054	0.0022	0.0023
2011	79.0832	20.9082	0.0045	0.0013	0.0028
2012	49.2093	50.7821	0.0050	0.0009	0.0027
2013	48.0390	51.9528	0.0046	0.0009	0.0027
2014	26.5207	73.4721	0.0040	0.0009	0.0023
2015	38.3205	61.6686	0.0068	0.0009	0.0032
2016	49.5976	40.3947	0.0036	0.0009	0.0032
2017	44.4058	55.5864	0.0028	0.0019	0.0031
2018	84.6401	15.3514	0.0046	0.0009	0.0030
2019	82.1312	17.8615	0.0042	0.0004	0.0027
2020	31.3157	68.6720	0.0038	0.0002	0.0083

as 2011, 2018, and 2019, the basin still experienced mild drought in the northern and northeastern regions. According to the drought frequency histogram (Fig. 7), more than 80% of the total area experienced drought with 7, 8, 9, and 10 frequencies, indicating long-term mild drought in the basin. Long-term drought can be very harmful to water resources, agriculture, forestry, buildings, industry, and tourism.

LST anomalies and precipitation anomalies were calculated to determine their correlation with the NDVI anomaly. The PCC illustrated a positive correlation between the NDVI anomaly and mean precipitation anomaly ( $r = 0.42$ ) and a negative correlation between the NDVI anomaly and LST anomaly ( $r = -0.68$ ). The results indicated that the temperature anomalies had more substantial effects on the drought in

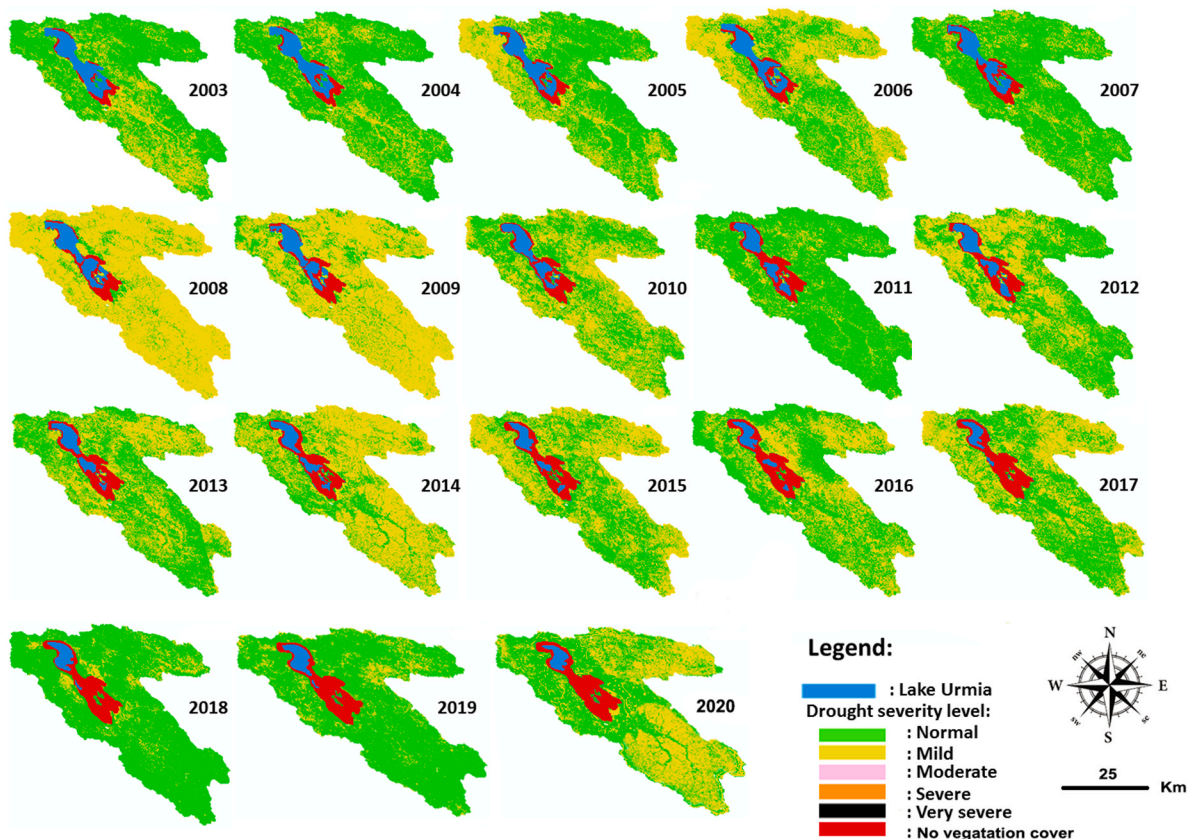


**Fig. 5.** The spatial pattern of drought severity in the Lake Urmia Basin during the growing seasons.

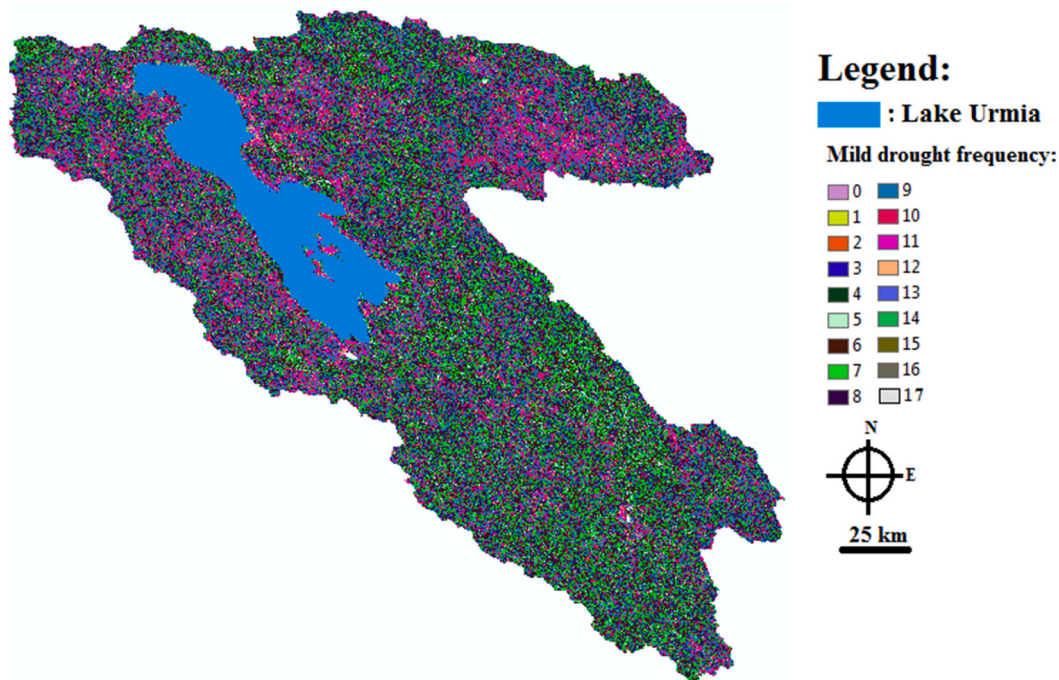


Fig. 6. Mild drought frequency map during the growing seasons 2003–2020 in the Lake Urmia Basin.

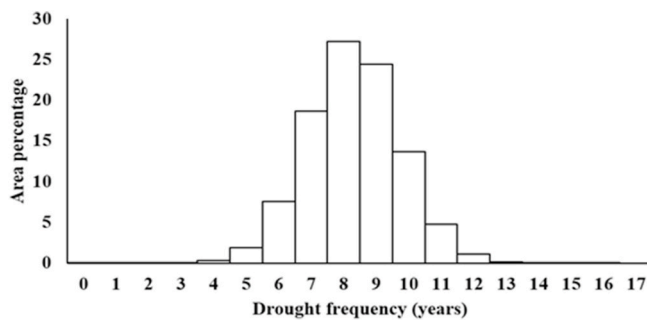


Fig. 7. Drought frequency histogram.

the basin. Some pixels in the northern parts of the map received more precipitation, with higher temperatures than the other pixels, and they showed more drought frequency in the study years. The reason for this is related to the fact that with higher temperatures, more evaporation occurred. While this produces more air moisture, all increased humidity does not fall over the same region, which leads to dry surfaces and contributes to the duration of droughts. Although the pixels located in the southern parts of the basin showed high LST and fewer precipitation values, they had less drought frequency than the pixels located in the northern parts of the basin. There are four large rivers in the southern part of the basin that have more than 65% inflow contribution to the lake, and the rivers provided sufficient water to support a significant amount of the land even during droughts.

The stronger PCC between drought conditions and the temperature anomaly than the precipitation anomaly indicated that the main reason for the mild drought conditions in the basin was the temperature anomaly. According to the results, while a long-term drought occurred in some parts of the basin from 2003 to 2017 and affected the lake, the Lake Urmia basin has never experienced harsh drought conditions during the past 17 years. In 2018 and 2019, when the basin experienced normal conditions, the LL was almost stable and even increased in some months; however, in the other years with wet conditions, such as 2007 and 2011, the LL was still decreasing. It could be concluded that drought

had essential impacts on the LL, although it was not the main reason for the decline.

### 3.3. Trend analytical results

Potential hydrologic and atmospheric trends in the basin were investigated at a monthly timescale to find traces of climate change. First, the lag-one autocorrelation coefficient of the hydro-environmental time series was computed to determine the significance of autocorrelation in each dataset. Table 3 presents the results of the analysis; additionally, correlograms were used to find autocorrelations (examples are given in Fig. 8). Long-term trends in the variables show climate-driven variations and provide information on hydrologic and atmospheric characteristics of the basin.

The correlograms indicate various powerful lags in the time series. High lag-1 values show that the MK2 trend test should be applied to study potential trends in the time series. Autocorrelation with a 12-month time lag indicates high seasonality patterns in the time series, which is an indicator that wavelet approaches should be employed to investigate the time series. Seasonality patterns are the specific features of some hydroclimatological variables such as precipitation and temperature.

The MK tests indicated a statistically significant decreasing trend in the LL dataset (Z-value = -3.61). Accordingly, there was no meaningful trend in precipitation time series (Z-value = -0.25) in the basin, which

Table 3  
Lag-one autocorrelation of the variables.

Variable	Lag-one	Z-value
LST	<b>0.8314</b>	1.4941
NDVI	0.6570	<u>2.5972</u>
ET	<b>0.7173</b>	<u>2.7327</u>
Precipitation	<b>0.4239</b>	-0.2587
LL	<b>0.8917</b>	<u>-3.6165</u>
SM	<b>0.7947</b>	0.8427

\* The **bold** values indicate a statistically significant autocorrelation; therefore, MK2 was used to study their trends.

\* Underlined values have statistically significant trends.



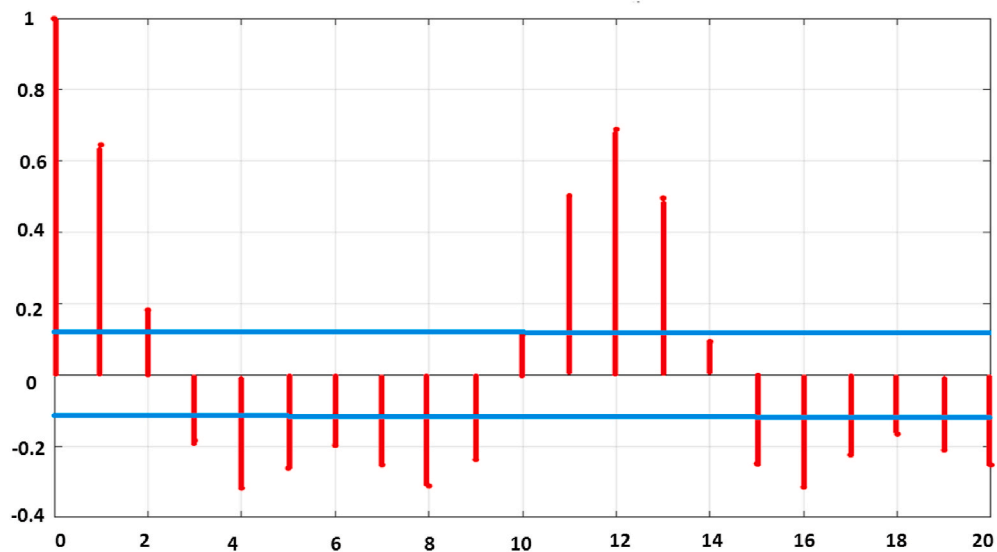


Fig. 8. The correlograms of the NDVI time series.

indicates that precipitation was not the primary reason for the LL decline. The Z-value of the SM ( $=0.84$ ) also indicated that there was no notable trend in the SM time series. In addition, the results showed that the LST time series did not have a significant positive trend (Z-value = 1.49) in the basin, which is an indicator of the unimportant role of increasing temperature in the problem. It is concluded that increasing the temperature did not have a considerable impact on the LL decline. The MK trend tests revealed a positive, statistically significant trend in the NDVI (Z-value = 2.59), which could be an indicator of expansion in agricultural and irrigation activities. The observed increasing trend in

the NDVI is consistent with recent literature that reported increasing water withdrawal and increasing agrarian activities in the basin (e.g., Ashraf et al., 2017; Chaudhari et al., 2018). Besides, the results are in alignment with general drought assessment in Iran which stated that Iran’s agriculture has expanded even in dry years (Maghrebi et al., 2020). On the other hand, ET rose with a significant trend (Z-value = 2.73) when precipitation and SM levels were generally stable. It is concluded from the fundamental water balance rule in a watershed that increased ET in the basin with steady precipitation, and SM conditions indicate decreasing runoff in the watershed and the lake’s inflow. This

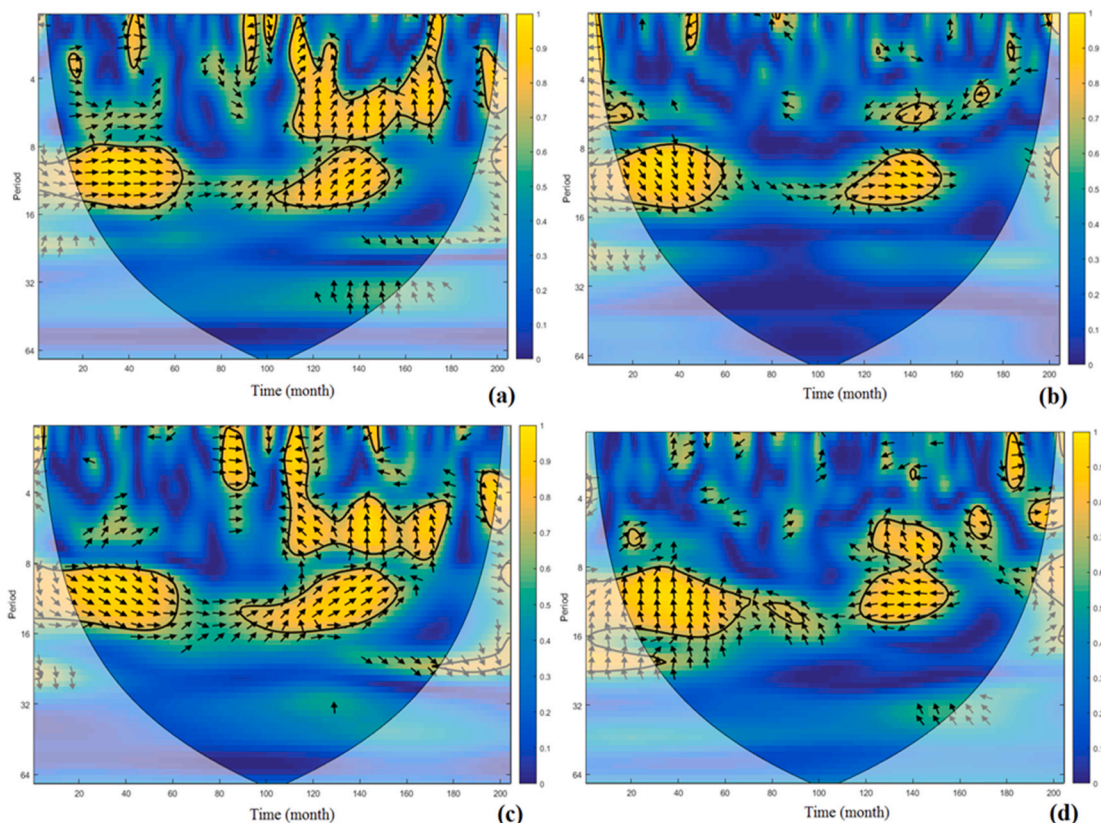


Fig. 9. Wavelet coherence between LL time series and (a) ET, (b) LST, (c) NDVI, and (d) precipitation time series.



fact was also reported in recent studies for other water resources in the world, such as Destouni et al. (2013) for the Aral Sea.

### 3.4. Results of correlation analysis

To further investigate the relationships between LL decline and variations in the hydrologic and atmospheric variables, correlation analysis was performed using WTC at a monthly scale. Fig. 9 (a) shows that the common periodicities between the LL time series and ET have an 8-16-month frequency band. The in-phase correlation from 2003 to 2011 can be observed in the graph. The 8-16-month frequency correlation between ET and LL stretched from 2003 to 2016; however, its significance was lower from 2008 to 2011 when, according to Fig. 4a, the LL did not experience a continuous decline. A quarter phase difference between the LL signal and ET time series from 2011 to 2016 in an 8-16-month period reveals that ET affects LL with a 2-4-month time lag. The time lag was in-phase, again, in the last months of this period, but from 2016 to 2019, its significance experienced a remarkable decline, which became strong again after early 2019. Significant deterioration should have an anthropogenic reason because nature-related processes are gradual processes. This decline coincided with the start of the new rules and policies of the government to control agricultural activities. According to Fig. 4a, from 2017 to 2019, the LL increased, and from 2019, it declined again. According to Fig. 9 (a), ET and LL have common periodicities in a 4-8-month frequency band, which was not significant in the first stage of the period, but from 2012 to 2018, it became statistically significant with a 1-2-month lag time when the LL was decreasing. The close correlation between ET and LL time series in various years, especially the years in which LL was declining and ET was increasing significantly, indicates that ET plays an important role in the LL decline of Lake Urmia.

The WTC between LST and LL (Fig. 9b) shows that there was a strong correlation with an 8-16-month frequency. The significant parts of the relationship shown in the graph (Fig. 9b) are almost in the years and frequencies as those for ET and LL in the WTC graph (Fig. 9a), which show a close relationship between ET and LST. High temperatures could intensify ET from the basin and evaporation from the lake's surface. Although the high temperature was one of the primary reasons for the high ET level, it was not the main reason in the basin because the increasing trend in the ET time series was much greater than that for temperature. In addition, ET showed some common periodicities with LL at various frequencies and years, but LST shared an 8-16-month frequency with LL, similar to ET.

According to Fig. 9 (c), the common periodicities between the LL and NDVI time series had an 8-16-month frequency band from 2003 to 2016 similar to ET. A quarter phase difference between the LL and NDVI time series from 2011 to 2016 in 8-16-month periods indicated that the vegetation cover affected LL with a 2-4-month time lag. The time lag was also the same as the time lag between ET and LL from 2011 to 2016. There was a significant correlation between the NDVI and LL in 4-8-month periodicities with a 2-4-month time lag from 2012 to 2018, which could also be seen between ET and LL. The same correlation between LL and ET and NDVI indicated that vegetation cover had a significant impact on ET. Moreover, the statistically significant positive trends in ET and NDVI datasets revealed in the previous section, as well as a close correlation in different years and periods between the ET and NDVI, showed that the increasing ET in the basin, which led to a decreasing LL, was an effect of increasing vegetation cover in the absence of sufficient precipitation and SM.

Regarding the WTC results between precipitation and LL (Fig. 9d), the common periodicities had an 8-16-month frequency band with a quarter phase difference from 2003 to 2009. It smoothly changed to anti-phase after 2013. A close correlation between precipitation and LL was seen in almost all years, which indicates a close relationship. According to the nonsignificant trend in the precipitation time series and its close correlation with LL in every month, it could be concluded that

although precipitation had a close relationship with LL, the precipitation problem did not have significant impacts on the LL decline of the lake.

The results of the WTC (Fig. 9) indicated that human land- and water-use impacts are obvious in the region. To confirm the results and perform more investigations in the region to determine the locations with significant agricultural expansion, NDVI maps between 2003 and 2020 were generated (Fig. 10).

Although there has always been heated debate among different provinces located in the basin (East Azerbaijan, West Azerbaijan, and Kurdistan) relating to the problem, Fig. 10 illustrates that human activities have impacted the entire basin. According to Fig. 10, the spatial distribution of the regions with dense vegetation cover changes between 2003 and 2020. To explore the landscape and identify the category of vegetation cover, a field investigation was performed, and the results validated that the regions were farmlands. The results of the fieldwork in addition to the RS map results indicate that agricultural expansion has occurred in all three provinces. According to the vegetation cover maps of 2003 and 2020 (Fig. 10), the highest value of NDVI in the basin was increased during the past 17 years. The growth in NDVI is an indicator of healthier vegetation cover. The denser vegetation cover in the basin in the situation that there is no increment in precipitation, is another indicator of growing anthropogenic activities in the basin.

## 4. Conclusions

Investigating the main reasons for the hydro-environmental problems of large saline lakes is a priority in studies related to water resources, the environment, hydrology, and climate change. The situation plays a crucial role in global change due to its effects on many natural processes. To determine the main reasons, drought indices and hydro-environmental factors in the Lake Urmia Basin, as the second-largest saline lake on Earth, were investigated in this study.

The results showed that the Lake Urmia Basin experienced long-term mild drought conditions from 2003 to 2018. Additionally, almost all other years have experienced drought situations, with more than 30% of

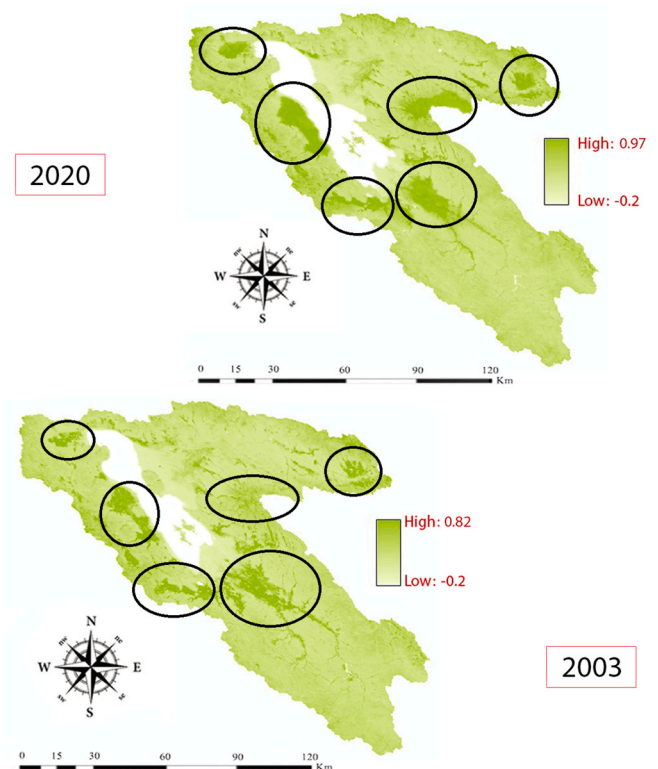


Fig. 10. NDVI maps of the Lake Urmia Basin (2020 and 2003).

the entire area. According to the results, the basin had only non-drought and mild drought conditions and did not experience severe droughts. It is concluded that drought condition could have intensified the LL decline but it could not be the significant reason. The annually changing condition of drought in the basin is also an indicator of anthropogenic activities that affect the environment.

The trend analysis of the hydroclimatological and LL time series showed a considerable decreasing trend in the LL time series. The increasing trend in the NDVI and ET time series based on stable precipitation, LST, and SM indicated that anthropogenic activities in the basin are the main reason for the problem. The WTC results showed the common periodicities between the LL and hydroclimatological time series. According to the main periodicities, it was concluded that the main reason for increasing ET in the basin was increasing vegetation cover in terms of agricultural activities, which led to the LL decline of the lake. At the next stage, the NDVI maps of 2003 and 2020 were visually compared, and a field investigation was performed to confirm the results of the WTC and to determine the main locations of excessive water usage. The conclusion is that agricultural expansion has occurred in all three provinces in the basin.

The results of this study are a call to action for water resource managers and people to consider water-related and water-induced problems in their water-utilization programs. Studying groundwater and surface waters in the basin using the same approaches may improve the results of future studies, which were limitations in the current study due to data scarcity. Large saline lakes have various problems worldwide, including lake-level decline, and human water and land use are among the main reasons for a great number of issues. Depletion of water resources will cause human health, economic, and habitat problems not only in this region but also all over the world.

#### CRediT authorship contribution statement

**Ehsan Foroumandi:** Project administration, Methodology, Writing – original draft. **Vahid Nourani:** Conceptualization, Supervision, Methodology, Writing – review & editing. **Sameh Ahmed Kantoush:** Validation, Formal analysis, Writing – review & editing.

#### Declaration of competing interest

The authors declare that they have no known competing financial interests or personal relationships that could have appeared to influence the work reported in this paper.

#### Acknowledgment

This work was funded by APN “Asia-Pacific Network for Global Change Research” under project reference number CRRP2020-09MY-Kantoush (Funder ID: <https://doi.org/10.13039/100005536>).

#### References

- Alivernini, M., Lai, Z., Frenzel, P., Fürstenberg, S., Wang, J., Guo, Y., Peng, P., Haberzettl, T., Börner, N., Mischke, S., 2018. Late quaternary lake level changes of Taro Co and neighbouring lakes, southwestern Tibetan Plateau, based on OSL dating and ostracod analysis. *Global Planet. Change* 166, 1–18. <https://doi.org/10.1016/j.gloplacha.2018.03.016>.
- Amirataee, B., Montaseri, M., Rezaie, H., 2018. Regional analysis and derivation of copula-based drought Severity-Area-Frequency curve in Lake Urmia basin, Iran. *J. Environ. Manag.* 206, 134–144. <https://doi.org/10.1016/j.jenvman.2017.10.027>.
- Ashraf, B., Aghakouchak, A., Alizadeh, A., Mousavi Baygi, M., Moftakhari, H.R., Mirchi, A., Anjileli, H., Madani, K., 2017. Quantifying anthropogenic stress on groundwater resources. *Sci. Rep.* 7, 1–9. <https://doi.org/10.1038/s41598-017-12877-4>.
- Chaudhari, S., Felfelani, F., Shin, S., Pokhrel, Y., 2018. Climate and anthropogenic contributions to the desiccation of the second largest saline lake in the twentieth century. *J. Hydrol.* 560, 342–353. <https://doi.org/10.1016/j.jhydrol.2018.03.034>.
- Danandeh Mehr, A., Hrnjica, B., Bonacci, O., Torabi Haghighi, A., 2021. Innovative and successive average trend analysis of temperature and precipitation in Osijek, Croatia. *Theor. Appl. Climatol.* 145, 875–890. <https://doi.org/10.1007/s00704-021-03672-3>.
- Danandeh Mehr, A., Vaheddoost, B., 2020. Identification of the trends associated with the SPI and SPEI indices across Ankara, Turkey. *Theor. Appl. Climatol.* 139, 1531–1542. <https://doi.org/10.1007/s00704-019-03071-9>.
- Dehghanipour, A.H., Panahi, D.M., Mousavi, H., 2020. Effects of Water Level Decline in Lake Urmia, Iran, Water (Switzerland).
- Delju, A.H., Ceylan, A., Pigué, E., Rebetez, M., 2013. Observed climate variability and change in Urmia lake basin, Iran. *Theor. Appl. Climatol.* 111, 285–296. <https://doi.org/10.1007/s00704-012-0651-9>.
- Destouni, G., Jaramillo, F., Prieto, C., 2013. Hydroclimatic shifts driven by human water use for food and energy production. *Nat. Clim. Change* 3, 213–217. <https://doi.org/10.1038/nclimate1719>.
- Elsanabary, M.H., Khafagy, H.E., Abdellah, S.E., 2021. Rainfall variation over Sinai Peninsula and its teleconnection to El Niño sea surface temperature. *J. Arid Environ.* 193, 104581. <https://doi.org/10.1016/j.jaridenv.2021.104581>.
- Fathian, F., Dehghan, Z., Eslamian, S., 2014. Analysis of water level changes in Lake Urmia based on data characteristics and non-parametric test. *Int. J. Hydrol. Sci. Technol.* 4, 18–38. <https://doi.org/10.1504/IJHST.2014.064398>.
- Figueira Branco, E.R., Rosa dos Santos, A., Macedo Pezzopane, J.E., Banhos dos Santos, A., Alexandre, R.S., Bernardes, V.P., Gomes da Silva, R., Barbosa de Souza, K., Moura, M.M., 2019. Space-time analysis of vegetation trends and drought occurrence in domain area of tropical forest. *J. Environ. Manag.* 246, 384–396. <https://doi.org/10.1016/j.jenvman.2019.05.097>.
- Foroumandi, E., Nourani, V., Sharghi, E., 2021. Climate change or regional human impacts? Remote sensing tools, artificial neural networks, and wavelet approaches aim to solve the problem. *Nord. Hydrol* 52, 176–195. <https://doi.org/10.2166/nh.2020.112>.
- Fujihara, Y., Tanakamaru, H., Tada, A., Ahmed Adam, B.M., Eltaib Elamin, K.A., 2020. Analysis of cropping patterns in Sudan's gash spate irrigation System using landsat 8 images. *J. Arid Environ.* 173, 104044. <https://doi.org/10.1016/j.jaridenv.2019.104044>.
- Grinsted, A., Moore, J.C., Jevrejeva, S., 2004. Application of the cross wavelet transform and wavelet coherence to geophysical time series. *Nonlinear Process Geophys.* 11, 561–566. <https://doi.org/10.5194/npg-11-561-2004>.
- Hassanzadeh, E., Zarghami, M., Hassanzadeh, Y., 2012. Determining the main factors in declining the Urmia lake level by using System dynamics modeling. *Water Resour. Manag.* 26, 129–145. <https://doi.org/10.1007/s11269-011-9909-8>.
- Keikhosravi Kiany, M.S., Masoodian, S.A., Balling, R.C., Montazeri, M., 2020. Evaluation of the TRMM 3B42 product for extreme precipitation analysis over southwestern Iran. *Adv. Space Res.* 66, 2094–2112. <https://doi.org/10.1016/j.asr.2020.07.036>.
- Khazaei, B., Khatami, S., Alemohammad, S.H., Rashidi, L., Wu, C., Madani, K., Kalantari, Z., Destouni, G., Aghakouchak, A., 2019. Climatic or regionally induced by humans? Tracing hydro-climatic and land-use changes to better understand the Lake Urmia tragedy. *J. Hydrol.* 569, 203–217. <https://doi.org/10.1016/j.jhydrol.2018.12.004>.
- Lashkari, A., Irannezhad, M., Zare, H., Labzovskii, L., 2021. Assessing long-term spatio-temporal variability in humidity and drought in Iran using Pedj Drought Index (PDI). *J. Arid Environ.* 185, 104336. <https://doi.org/10.1016/j.jaridenv.2020.104336>.
- Liu, S., Huang, S., Huang, Q., Xie, Y., Leng, G., Luan, J., Song, X., Wei, X., Li, X., 2017. Identification of the non-stationarity of extreme precipitation events and correlations with large-scale ocean-atmospheric circulation patterns: a case study in the Wei River Basin, China. *J. Hydrol.* 548, 184–195. <https://doi.org/10.1016/j.jhydrol.2017.03.012>.
- Liu, S., Huang, S., Xie, Y., Wang, H., Huang, Q., Leng, G., Li, P., Wang, L., 2019. Spatial-temporal changes in vegetation cover in a typical semi-humid and semi-arid region in China: changing patterns, causes and implications. *Ecol. Indic.* 98, 462–475. <https://doi.org/10.1016/j.ecolind.2018.11.037>.
- Maghrebi, M., Noori, R., Bhattarai, R., Mundher Yaseen, Z., Tang, Q., Al-Ansari, N., Danandeh Mehr, A., Karbassi, A., Omidvar, J., Farnoush, H., Torabi Haghighi, A., Kløve, B., Madani, K., 2020. Iran's agriculture in the anthropocene. *Earth's Futur* 8. <https://doi.org/10.1029/2020EF001547>.
- Mallick, J., Talukdar, S., Alsubih, M., Salam, R., Ahmed, M., Kahla, N. Ben, Shamimuzzaman, M., 2021. Analysing the trend of rainfall in Asir region of Saudi Arabia using the family of Mann-Kendall tests, innovative trend analysis, and detrended fluctuation analysis. *Theor. Appl. Climatol.* 143, 823–841. <https://doi.org/10.1007/s00704-020-03448-1>.
- Mischke, S., Liu, C., Zhang, J., Zhang, C., Zhang, H., Jiao, P., Plessen, B., 2017. The world's earliest Aral-Sea type disaster: the decline of the Loulan Kingdom in the Tarim Basin. *Sci. Rep.* 7, 1–8. <https://doi.org/10.1038/srep43102>.
- Moghim, S., 2018. Impact of climate variation on hydrometeorology in Iran. *Global Planet. Change* 170, 93–105. <https://doi.org/10.1016/j.gloplacha.2018.08.013>.
- Mullick, M.R.A., Nur, M.R.M., Alam, M.J., Islam, K.M.A., 2019. Observed trends in temperature and rainfall in Bangladesh using pre-whitening approach. *Global Planet. Change* 172, 104–113. <https://doi.org/10.1016/j.gloplacha.2018.10.001>.
- Nalley, D., Adamowski, J., Khalil, B., 2012. Using discrete wavelet transforms to analyze trends in streamflow and precipitation in Quebec and Ontario (1954–2008). *J. Hydrol.* 475, 204–228. <https://doi.org/10.1016/j.jhydrol.2012.09.049>.
- Nanzad, L., Zhang, J., Tuvdendorj, B., Nabil, M., Zhang, S., Bai, Y., 2019. NDVI anomaly for drought monitoring and its correlation with climate factors over Mongolia from 2000 to 2016. *J. Arid Environ.* 164, 69–77. <https://doi.org/10.1016/j.jaridenv.2019.01.019>.
- Nourani, V., Foroumandi, E., Sharghi, E., Dąbrowska, D., 2021. Ecological-environmental quality estimation using remote sensing and combined artificial intelligence techniques. *J. Hydroinf.* 23, 47–65. <https://doi.org/10.2166/hydro.2020.048>.

- Nyikadzino, B., Chitakira, M., Muchuru, S., 2020. Rainfall and runoff trend analysis in the Limpopo river basin using the Mann Kendall statistic. *Phys. Chem. Earth* 117, 102870. <https://doi.org/10.1016/j.pce.2020.102870>.
- Pettorelli, N., Viik, J.O., Mysterud, A., Gaillard, J.M., Tucker, C.J., Stenseth, N.C., 2005. Using the satellite-derived NDVI to assess ecological responses to environmental change. *Trends Ecol. Evol.* 20, 503–510. <https://doi.org/10.1016/j.tree.2005.05.011>.
- Rashid, M.M., Beecham, S., Chowdhury, R.K., 2015. Assessment of trends in point rainfall using Continuous Wavelet Transforms. *Adv. Water Resour.* 82, 1–15. <https://doi.org/10.1016/j.advwatres.2015.04.006>.
- Sobrino, J.A., Coll, C., Caselles, V., 1991. Atmospheric correction for land surface temperature using NOAA-11 AVHRR channels 4 and 5. *Remote Sens. Environ.* 38, 19–34. [https://doi.org/10.1016/0034-4257\(91\)90069-I](https://doi.org/10.1016/0034-4257(91)90069-I).
- Tong, S., Zhang, J., Bao, Y., Wurina, Terigele, Weilisi, Lianxiao, 2017. Spatial and temporal variations of vegetation cover and the relationships with climate factors in Inner Mongolia based on GIMMS NDVI3g data. *J. Arid Land* 9, 394–407. <https://doi.org/10.1007/s40333-017-0016-4>.
- Torrence, C., Compo, G.P., 1998. A practical guide to wavelet analysis. *Bull. Am. Meteorol. Soc.* 79, 61–78. [https://doi.org/10.1175/1520-0477\(1998\)079<0061:APGTWA>2.0.CO;2](https://doi.org/10.1175/1520-0477(1998)079<0061:APGTWA>2.0.CO;2).
- Wurtsbaugh, W.A., Miller, C., Null, S.E., Justin De Rose, R., Wilcock, P., Hahnenberger, M., Howe, F., Moore, J., 2017. Decline of the world's saline lakes. *Nat. Geosci.* 10, 816–821. <https://doi.org/10.1038/NGEO3052>.
- Ye, X.C., Liu, F.H., Zhang, Z.X., Xu, C.Y., 2020. Quantifying the impact of compounding influencing factors to the water level decline of China's largest freshwater lake. *J. Water Resour. Plann. Manag.* 146, 1–12. [https://doi.org/10.1061/\(ASCE\)WR.1943-5452.0001211](https://doi.org/10.1061/(ASCE)WR.1943-5452.0001211).
- Yue, S., Pilon, P., Phinney, B., Cavadias, G., 2002. The influence of autocorrelation on the ability to detect trend in hydrological series. *Hydrol. Process.* 16, 1807–1829. <https://doi.org/10.1002/hyp.1095>.
- Zhai, Y., Xia, X., Yang, G., Lu, H., Ma, G., Wang, G., Teng, Y., Yuan, W., Shrestha, S., 2020. Trend, seasonality and relationships of aquatic environmental quality indicators and implications: an experience from Songhua River, NE China. *Ecol. Eng.* 145, 105706. <https://doi.org/10.1016/j.ecoleng.2019.105706>.
- Zhang, Q., Xu, C.Y., Zhang, Z., Chen, Y.D., Liu, C.L., 2009. Spatial and temporal variability of precipitation over China, 1951–2005. *Theor. Appl. Climatol.* 95, 53–68. <https://doi.org/10.1007/s00704-007-0375-4>.
- Zhao, A., Yu, Q., Feng, L., Zhang, A., Pei, T., 2020. Evaluating the cumulative and time-lag effects of drought on grassland vegetation: a case study in the Chinese Loess Plateau. *J. Environ. Manag.* 261, 110214. <https://doi.org/10.1016/j.jenvman.2020.110214>.